

Chapter 3

Normalization for Effective Overburden Stress

3.1 Abstract

Effective overburden stress can have a significant influence on measured tip and sleeve resistance of the cone penetration test (CPT). For an accurate representation of tip and sleeve resistance it is essential to normalize these index measurements appropriately. A comprehensive study was conducted to review all aspects of CPT normalization, and to solidify normalization procedures for the CPT using both empirical results and theoretical analyses. This paper presents the results of this study in the form of an improved normalization scheme and its application.

3.2 Introduction

Raw CPT measurements can be misleading if effective overburden/confining stress effects are not taken into account. Low confining stresses that might be found at shallow depths, can result in a reduced measured tip and sleeve resistance. Whereas high confining stresses that might be found at greater depths, can result in a pronounced increase in measured tip and sleeve resistance.

Confining stress influences different soils differently. Cohesive soils respond to confining stress primarily as a function of over consolidation ratio (OCR) and undrained strength (s_u). Cohesionless soils respond to confining stress primarily as a function of

relative density (D_r) and the coefficient of lateral earth pressure (K_o), and to a lesser degree as a function of the angularity, compressibility, and crushing strength of the grains.

The effects of confining stress are nonlinear, showing a curve-linear decrease with linear increase in stress. To account for the effects of confining stress, the tip and sleeve resistance values are normalized to a reference stress value. The reference stress value that is convenient and commonly used in practice, is one atmosphere (1 atm. = 101.325 kPa = 1.033 kg/cm^2 = 14.696 psi = 1.058 tsf). One atmosphere is also a reasonable reference value because it is a median range of depth/pressure in geotechnical engineering problems.

3.3 Previous Research

The bulk of research on CPT normalization was conducted by Olsen et al. (1988, 1994, 1995a, and 1995b). Olsen (1994) utilized a technique of defining the normalization for tip and sleeve resistance of various soil types from field and laboratory data. For a given “uniform” soil strata the resistance was measured at different confining stresses. The results were plotted as a function of confining stress in log-log space, resulting in a linear relationship. The stress normalization exponent for that particular soil state is then the slope of the linear fit in log-log space (with the symbol c for tip exponent and s for sleeve exponent). This procedure was carried out for all soil types where reasonable data existed, which led to the Olsen & Mitchell, 1995 (Figure 3.1) normalization exponent contours. These exponent contours can then be used in a forward analysis to normalize

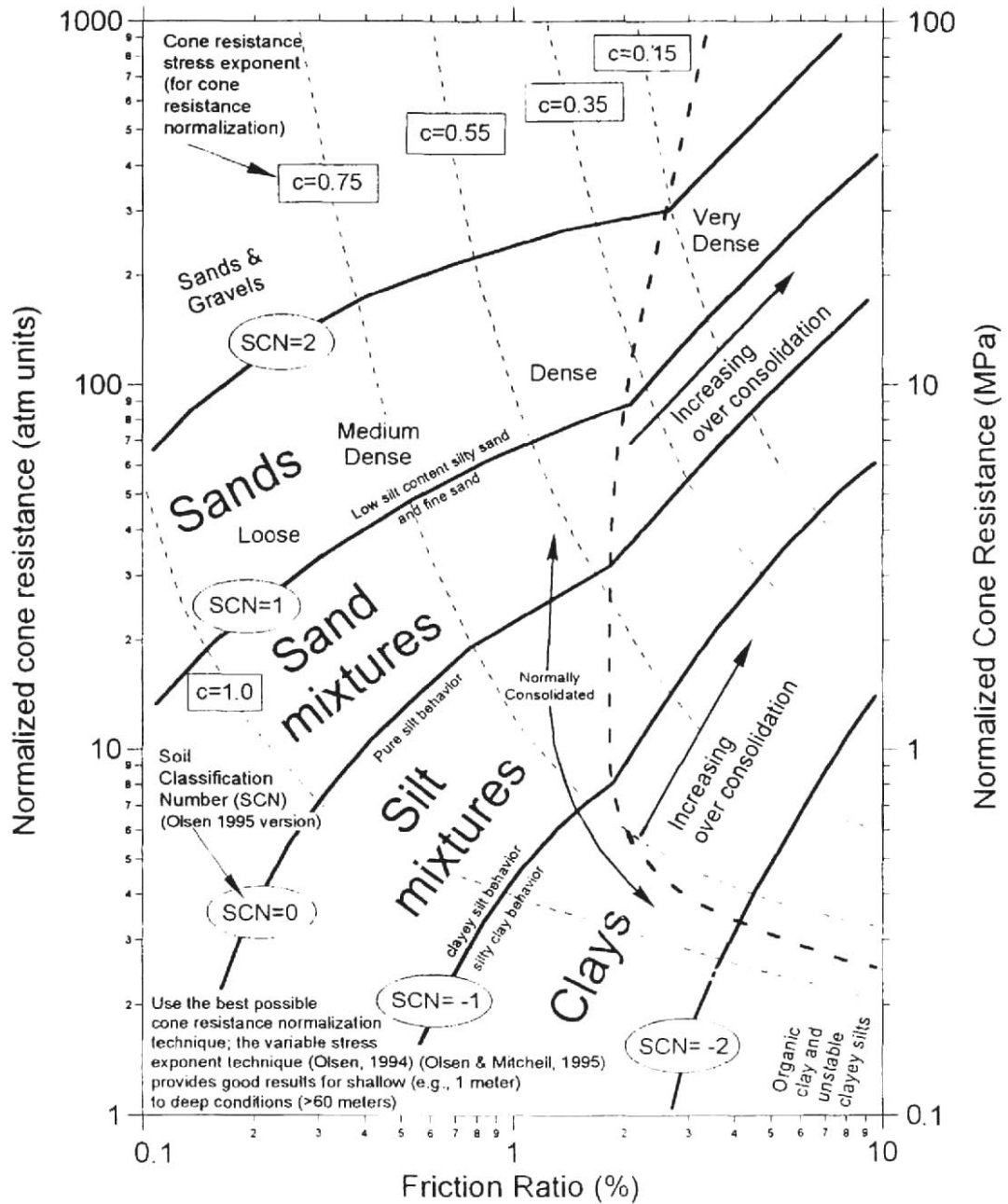


Figure 3.1 Variable CPT Normalization from Olsen & Mitchell (1995).

the tip and sleeve resistance as,

$$q_{c,1} = C_q \cdot q_c \text{ and } f_{s,1} = C_f \cdot f_s \quad (3.1)$$

$$\text{where } C_q = \left(\frac{P_a}{\sigma_v'} \right)^c \text{ and } C_f = \left(\frac{P_a}{\sigma_v'} \right)^s$$

This work incorporated over two decades of field data and an extensive database of chamber test studies to deduce the tip normalization for a number of different soil types. Olsen laid down the groundwork for cone normalization, and subsequent researchers (e.g. Robertson & Wride, 1998) deferred to this body of work when addressing normalization.

An inherent limitation in an empirical approach is that a layer must be uniform and cover a sufficient depth to be of use. Normalization data in granular materials is generally restricted to chamber test results because of the inherent variability in the field due to this type of depositional environment. In fine-grained soils, normalization data is generally restricted to field tests because of the difficulty of performing chamber studies on this type of soil. For soils that fall outside the requirements of uniformity and extent, it is difficult if not impossible to generate or retrieve normalization data for analysis.

Olsen (1994) used an extensive database (Figure 3.2, 3.3, and 3.4) to delineate the areas that were quantifiable, and interpolated and/or extrapolated elsewhere. Olsen's characterization chart, Figure 3.1, shows variable tip normalization exponents for different soil types, with sleeve normalization exponents assumed to be equivalent to tip.

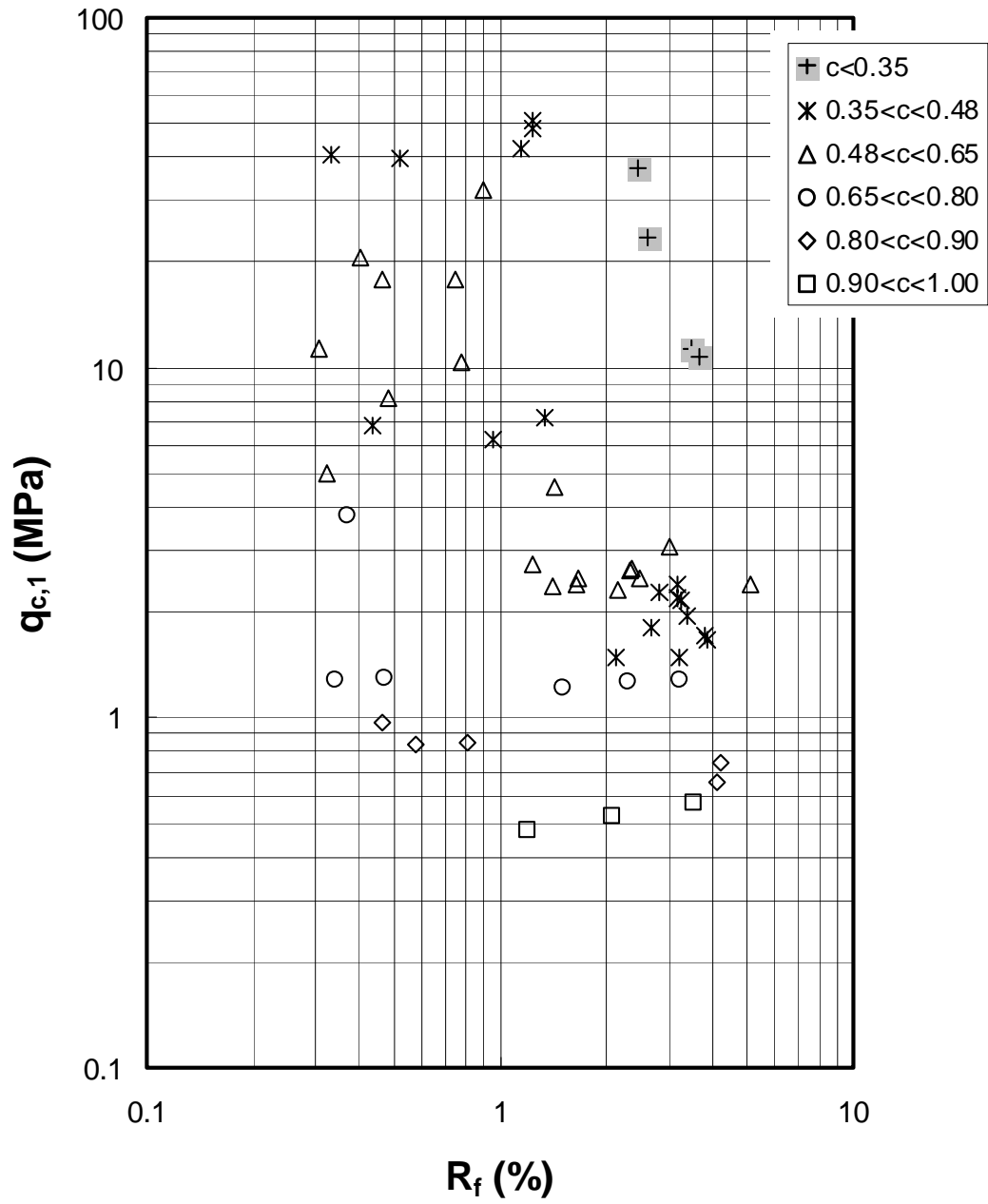


Figure 3.2 Tip Normalization Exponent Results from Field Data (after Olsen, 1994).

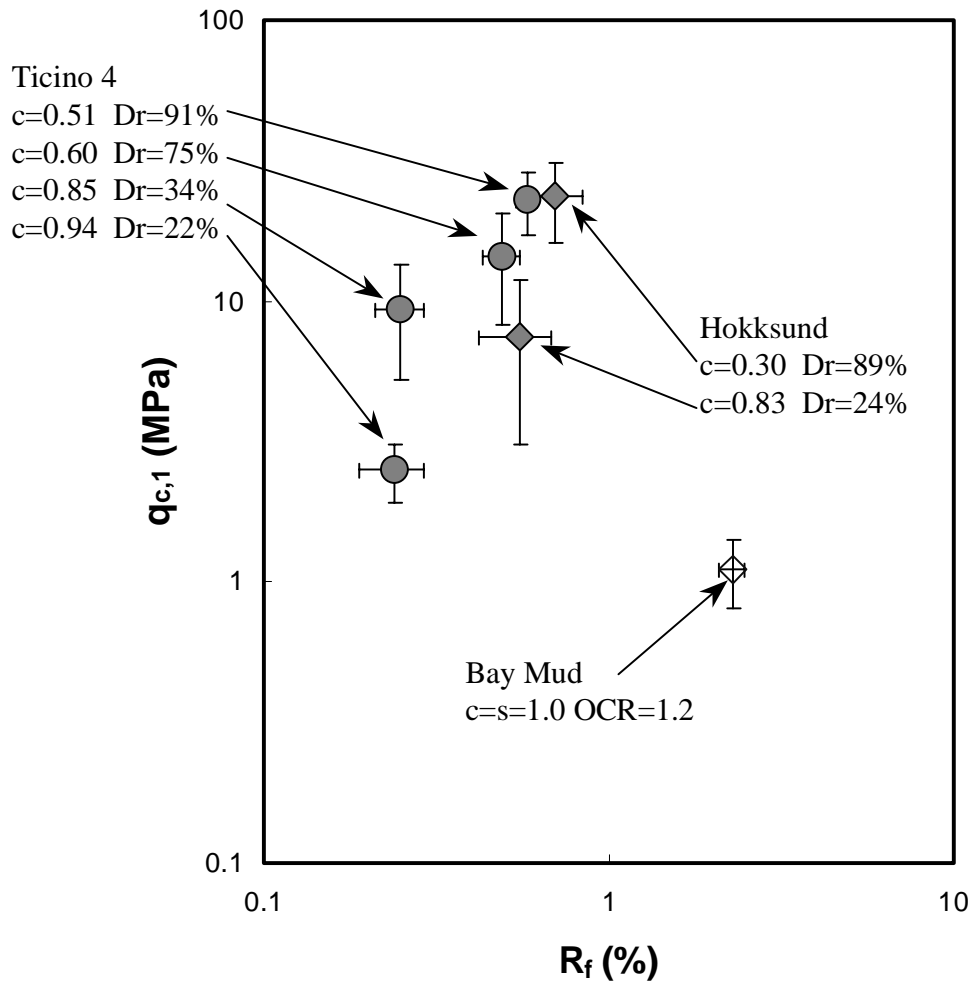


Figure 3.3 Tip Normalization Exponent Results from 57 Calibration Chamber Tests and Bay Mud Field Data (after Olsen, 1994).

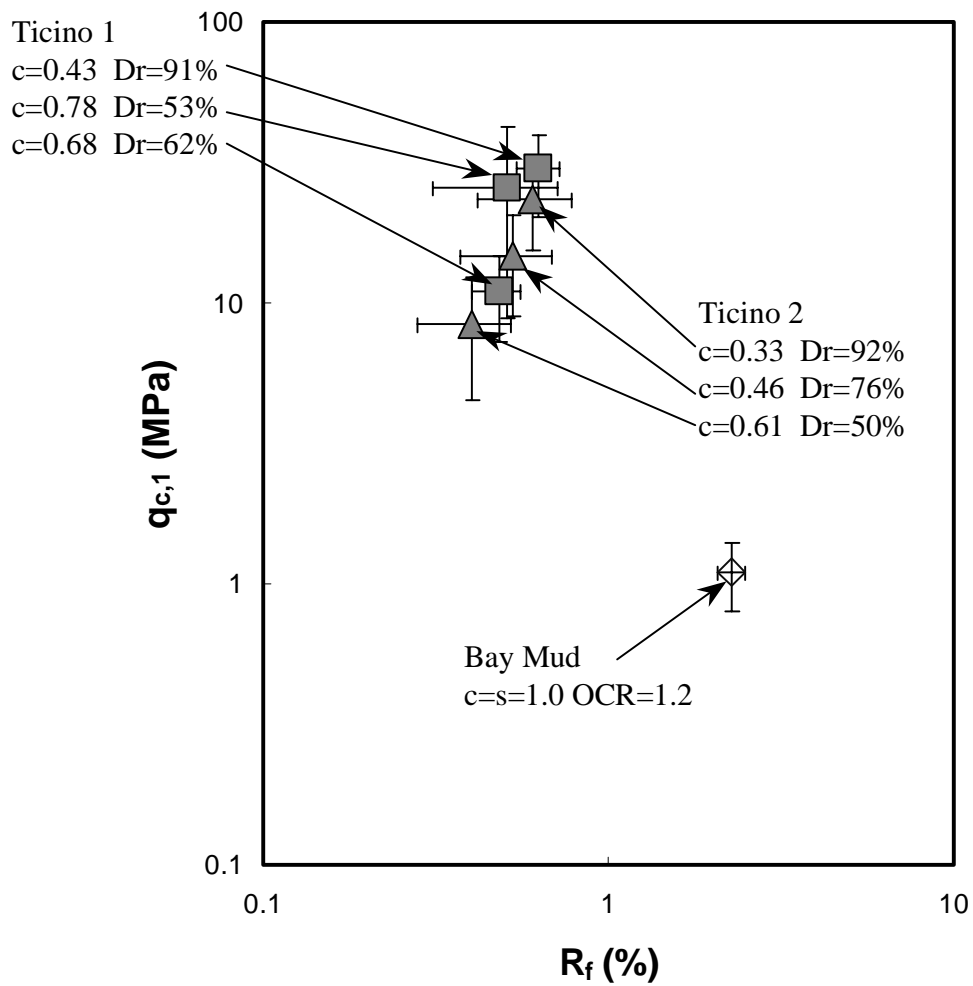


Figure 3.4 Tip Normalization Exponent Results from 25 Calibration Chamber Tests and Bay Mud Field Data (after Olsen, 1994).

3.4 Theoretical Foundation for Normalization

To expand on Olsen's pioneering work a new approach was in order. This approach was to look at a theoretical foundation for CPT normalization. A review of methods that theoretically predict CPT measurements from fundamental soil properties was carried out. There are many methods that have been proposed, including; bearing capacity, cavity expansion, strain path, steady state, incremental finite element, and discrete element.

Based on the literature (Mayne, 1991; Keaveny, 1985, Keaveny & Mitchell, 1986; Yu & Houlsby, 1991; Salgado, 1993; Collins et al., 1994; Huang & Ma, 1994; Salgado et al., 1997; Yu & Mitchell, 1998; Yu, 2000) cavity expansion methods are the most advanced for theoretical CPT tip predictions. Yu & Mitchell (1998), in particular, looked at all theoretical methods that were functionally comparative at the time and found cavity expansion to be the most developed as well as providing the greatest accuracy in CPT predictions over all stress ranges. Bearing capacity methods are only valid for shallow or low confining stress regimes, and provide a linear approximation to a nonlinear problem. Other methods such as steady state, discrete element, strain path, and incremental finite element are promising methods but are in their infancy and may only predict CPT tip resistance for a specific soil type and stress condition. Steady state methods were used in this study as qualitative support for the quantitative cavity expansion results.

Bishop et al. (1945) was the first to note the analogy between the expansion of a cavity and the penetration of a cone in an elastic medium. Subsequent researchers developed

this further by incorporating higher order stress-strain relationships to model sands and clays with increasing rigor and accuracy (Vesic, 1972; Ladanyi & Johnston, 1974; Baligh, 1976; Carter et al., 1986; Yu & Houlsby, 1991; Collins et al., 1992; Salgado et al., 1997).

Cavity expansion methods require two steps; (1) a theoretical (analytical or numerical) cavity limit pressure solution is calculated, and (2) this limit pressure is then related to the cone tip resistance. This research utilizes various cavity expansion solutions to determine normalization exponents. Because of the complexity of soil behavior and the different solutions required for different types of soil behavior, the discussion of theoretical methods is divided into four soil state categories; cohesive normally consolidated, cohesive overconsolidated, cohesionless contractive, cohesionless dilatant.

3.4.1 Cohesive Normally Consolidated

Yu & Houlsby (1991) derived an analytical solution for a total stress cylindrical cavity expansion model in normally consolidated cohesive clay. The soil is modeled as a linear elastic-perfectly plastic material using a Mohr-Coulomb yield criterion. The closed form solution for a standard 60 degree cone, with a perfectly rough surface is:

$$q_c = N_c \cdot s_u + \sigma_m \quad (3.2)$$

$$\text{where } N_c = 9.4 + 1.155 \cdot \ln \frac{\sqrt{3} G}{2 s_u} = \text{cone factor}$$

and s_u = undrained strength and σ_m = mean total stress

Yu & Mitchell (1998) showed that this solution gave good results when compared to empirical data and other analytical solutions.

For this study, Yu's closed form solution (Equation 3.2) was calibrated using chamber data from Kurup et al. (1994). The elastic shear modulus, G , was calculated using the equation for G_{max} from Hardin (1978) and a reasonable value of shear strain. This solution was then used to predict tip resistance, using a CL/CH model clay soil, with an OCR=1.0, for a variety of stiffness indices under different confining stresses. The normalization exponent from the results was $c \cong 1.0$.

Currently there is no analytical solution for sleeve resistance. Sleeve resistance (f_s) is a function of the effective remolded strength (δ_r) and the effective horizontal pressure (σ_h').

$$f_s \propto \sigma_h' \tan \delta_r \quad (3.3)$$

The effective horizontal pressure can be thought of as a cylindrical cavity expansion limit pressure for sleeve resistance measurements (Keaveny, 1985; Keaveny & Mitchell, 1988; Masood, 1990; Masood & Mitchell, 1993). Kurup et al. (1994) chamber data was used to correlate tip and sleeve resistance through a form of Equation 3.3. This was then used to approximate the corresponding sleeve resistance.

Using the steady state method for cohesive normally consolidated soils, Yu et al. (2000b) showed that tip resistance and friction ratio have similar trends as a function of stiffness index, which is itself a function of confining stress. Showing that both tip and sleeve can be founded in cylindrical cavity expansion methods, and both are a function of the stiffness index, and normalization being a function of the cone's response to confining stress, then it is hypothesized that the tip and sleeve are normalized equivalently for cohesive normally consolidated soils.

3.4.2 Cohesive Overconsolidated

For this soil state, the cavity expansion model must have a constitutive relationship that captures undrained cohesive soil behavior accurately. Researchers have addressed this soil state with varying success (Mayne, 1991; Collins & Yu, 1996). Cao et al. (2001) and Chang et al. (2001) published companion papers that developed a closed form modified Cam clay cavity expansion model that can be used to predict tip resistance. These papers were also bolstered by discussions from Ladanyi (2002) and Mayne et al. (2002). This spherical cavity model is shown in its simplified form below:

$$q_c = \frac{4}{3} \cdot \alpha_\epsilon \cdot s_u \cdot \left(\ln \left(\frac{G}{s_u} \right) + 1 \right) + \sigma_m \quad (3.4)$$

where α_ϵ = strain rate factor = 1.64 for 10 cm² cones

The cavity limit pressure equation, the basis for Equation 3.4, was compared with the solution proposed by Yu & Collins (1996). Cao et al. (2001) used a small strain assumption in the derivation of their closed form solution, whereas Collins & Yu (1996) used a large strain assumption for their numerically generated solution. The two methods compare favorably. The cone predictive form of this cavity expansion model (Equation 3.4) was compared to both laboratory and field data and shown to agree reasonably well (Chang et al., 2001).

The Chang et al. (2001) cavity model results indicate that OCR has only a small effect on predicted tip resistance. Yu et al. (2000b) included some preliminary analysis on overconsolidated soils using their steady state model and also found that OCR had little effect on the predicted tip resistance. Based on the trends observed in the normally consolidated cohesive soils it is hypothesized that overconsolidated soils behave in a similar fashion, and that tip and sleeve normalize equivalently.

To confirm this, field data of young bay mud from the San Francisco Bay, was used to calculate normalization exponents for the tip and sleeve. The young bay mud is slightly overconsolidated ($OCR \cong 1.2$) and deposited in relatively homogenous layers of sufficient thickness to extract the response of tip and sleeve resistance for varying confining pressures. The results indicate an equivalent normalization exponent for the tip and sleeve (Figures 3.3 and 3.4).

3.4.3 Cohesionless Contractive

Ladanyi & Johnston (1974) derived an analytical solution for tip resistance in contractive sands using a spherical cavity approach and a linear elastic-plastic von Mises failure criterion.

$$q_c' = N_q \cdot \sigma_{v0}' \quad (3.5)$$

$$\text{where } N_q = \frac{(1 + 2K_0)A}{3} \left[1 + \sqrt{3} \tan(\lambda\phi') \right]$$

The variable A is the ratio of the effective spherical cavity limit pressure to the initial mean effective stress, which is a function of strength and stiffness. There is no closed form solution for A, it must be calculated numerically. Yu (2001) developed a numerical solution, implemented in the code CAVEXP, for calculating the spherical cavity limit pressures required to determine A. The combination of Yu's numerical solution for the limit pressure and Ladanyi & Johnston's analytical solution for the relation between that limit pressure and tip resistance compares quite favorably with empirical results (Yu & Mitchell, 1998).

The combination of the Ladanyi & Johnston's (1974) analytical solution and the Yu (2001) numerical solution for limit pressures was calibrated using chamber test data of various sands from Salgado's (1993) exhaustive compendium. The calibrated model was then used to predict tip resistance and tip normalization exponents.

As with the cohesive soils, there is currently no theoretical solution for sleeve resistance. The sleeve resistance is a function of the horizontal effective stress and an effective modified friction angle, which is analogous to the tip resistance;

$$f_s \propto \sigma_h' \tan \phi' \quad (3.6)$$

However, sleeve resistance is assumed to be based on cylindrical cavity expansion geometry. One difference between tip and sleeve resistance is a function of the ratio of limit pressures for a cylinder versus a sphere ($1:\pi h^2$). Collins et al. (1994) included in their research the differences in using cylindrical versus spherical cavity geometries derived for sands. Their results concur that there is a divergence of the tip and sleeve exponent for the contractive soil state in granular materials.

Chamber tests were used to calibrate a form of Equation 3.6 and sleeve resistance values were then approximated, to correlate with the predicted tip resistance values.

3.4.4 Cohesionless Dilatant

Salgado (1993) developed a nonlinear elastic-plastic cavity expansion model that accounts for dilatant behavior in granular material. This model requires a finite element solution for the cavity limit pressure, which has been implemented in the code CONPOINT (Salgado et al., 1997 and 2001). Accounting for this soil state, Salgado's model first numerically calculates the cylindrical cavity limit pressure, then uses a stress rotation analysis to obtain the tip resistance. Salgado's model follows the formulation,

$$q_c = 2 p_v e^{\pi \tan \phi_r} \frac{(1 + C)^{1+\beta} - (1 + \beta)C - 1}{C^2 \beta(1 + \beta)} \quad (3.7)$$

where the independent variables in this equation are described in Salgado (1997). This model has been shown to agree well with empirical data by Yu & Mitchell (1998).

Boulanger (2003) used Salgado's model as a theoretical basis to calculate normalization exponents for materials subjected to high confining stresses ($\sigma_v' > 4$ atm) and cyclic loads. Chamber test results from Salgado (1993), for samples of $D_r = 0.75-0.85$ and $\sigma_v' > 4$ atm (as corresponding to Boulanger's analysis) were used to locate the normalization exponent range in R_f versus $q_{c,1}$ space with the other cavity expansion model results. There is good agreement with Boulanger's analysis and the other techniques used in this study, as can be seen in Figure 3.5.

Mitchell and Keaveny (1986) took an approach that returned to the seminal work in analytical cavity expansion solutions by Vesic (1972). Their results show that for soils of high compressibility (low I_{rr}), a spherical cavity model predicted tip resistance best. This agrees with the cohesionless contractive results using the Ladanyi & Johnston's (1974) closed form solution with Yu's (2001) numerical cavity limit pressure code. The corollary is a low compressibility soil (high I_{rr}), which was shown to agree best with a cylindrical cavity model.

Again, assuming that the sleeve resistance is based on cylindrical cavity expansion, the above results would indicate that there is minimal divergence of the tip and sleeve normalization exponent for dilatant granular soils. However, dilatant soils will tend to arch at the trailing edge of the tip. This can lead to a higher horizontal effective stress for the tip than for the sleeve. This would suggest a divergence of tip and sleeve normalization exponents with increased dilatancy.

3.4.5 Cavity Expansion Results

The results from the cavity expansion analyses are presented in Figure 3.6, a plot of the calculated tip normalization exponents over their $q_{c,1}$ and R_f ranges. The model results were generated for an effective stress range of 0.5 to 3.0 atm, with the exception of Boulanger's (2003) model that was derived for effective stress values higher than 4.0 atm.

3.5 Sleeve Normalization

The evaluation of sleeve normalization presents a more elusive problem because there are currently no theoretical solutions for predicting sleeve resistance. The sleeve predictions so far presented have been based on rough assumptions in order to approximate sleeve resistances that correspond to the theoretically derived tip resistances. These approximations have been calibrated using chamber data but lack the consistent and rigorous treatment that tip resistance has received.

Olsen, in his compilation of field and laboratory data scrutinized normalization exponents for sleeve resistance. Shown in Fig. 3.7, is the results of Olsen's analysis, with the ratio of sleeve and tip normalization exponents versus normalized sleeve resistance. Olsen presented the data in this manner because it provided the best linear correlation out of different variable combinations. This trend shows the nonlinear relationship between tip and sleeve normalization exponents. Based on the lack of conclusive results, Olsen recommended equivalent tip and sleeve exponents, which for most applications only slightly alters the results.

Based on the qualitative analysis from the different soil states presented thus far, and on the data from Olsen's work, a preliminary representation of sleeve exponent curves, in relation to tip exponent curves, is presented in Figure 3.8. The curves do diverge in certain regions of the chart. When normalizing the tip and sleeve resistance for use in soil characterization or other engineering applications, however, the difference between c and s becomes insignificant. For example, given raw cone measurements of $q_c=30$ MPa and $f_s=300$ kPa at 3 atm of effective overburden pressure, this gives an $R_f=1.0$. Note that these values lie in the region of Figure 3.8 where a large divergence of tip and sleeve resistance has been shown to occur. Now if we take $c=0.35$ and $s=0.40$ from the curves and normalize using Equation 3.1, to get $q_{c,1}=19.7$ and $f_{s,1}=185.4$, this give an $R_f=0.942$. The overall change in R_f is less than 6%, which is insignificant. Therefore, using equivalent normalization curves for both the sleeve and tip is reasonable.

3.6 Forward Normalization Analysis

New normalization curves have been developed using current theoretical techniques as shown in Figure 3.9. To normalize tip and sleeve appropriately, an iterative procedure is necessary. The raw tip and friction ratio are used to find an initial estimate of the normalization exponent. The tip is then normalized using this exponent (note: the friction ratio will not change when tip and sleeve are normalized equivalently). The normalized tip resistance and friction ratio values are then replotted and evaluated for how close they fall to the normalization exponent value used. An updated normalization exponent is selected and the procedure is repeated. This process usually requires only two iterations to converge.

To aid in computation, an approximation of the normalization exponent curves can be reduced to the equation,

$$c = f_1 \cdot \left(\frac{R_f}{f_3} \right)^{f_2} \quad (3.7)$$

$$\text{where } f_1 = x_1 \cdot q_c^{x_2}$$

$$f_2 = -(y_1 \cdot q_c^{y_2} + y_3)$$

$$f_3 = \text{abs}(\log(10 + qc))^{z_1}$$

$$\text{and } x_1 = 0.78, x_2 = -0.33, y_1 = -0.32, y_2 = -0.35, y_3 = 0.49, z_1 = 1.21$$

This equation has no physical significance other than it gives a good approximation of the tip normalization contours.

3.7 CPT Versus SPT Normalization

Variable normalization for confining stress effects on CPT measurements has been shown to be inherent in the *in situ* measuring process. The normalization exponent is an indicator of the soil's state under the given stress conditions. Use of a constant normalization exponent can lead to incorrect normalized values.

This error has also become evident in the normalization of SPT measurements where the exponent is taken as a constant for all soil types and stress conditions (usually around 0.5). Researchers in liquefaction engineering have noted this inaccuracy in the field data and chamber results, and have partially compensated for it by using the additional correction factor of K_σ (Seed, 1983; NCEER, 1997). Use of variable normalization exponents obviates the use of a K_σ when working with the CPT.

Currently there are no theoretical solutions for the SPT. This relegates critical analysis to chamber studies and field results. As the SPT tends to be a “non-standard” test, the variability of the results from different researchers and different equipment has the tendency to cloud the detail needed for assessing confining stress effects.

3.8 Summary and Conclusions

This paper presents the results of a comprehensive study of the normalization of CPT measurements for effective overburden stress effects. A review of previous field and calibration chamber results was conducted. A theoretical framework utilizing advances in cavity expansion analysis and steady state methods is presented. This framework gives greater confidence in a variable normalization procedure that is a function of soil state and produces accurately normalized CPT resistance values.

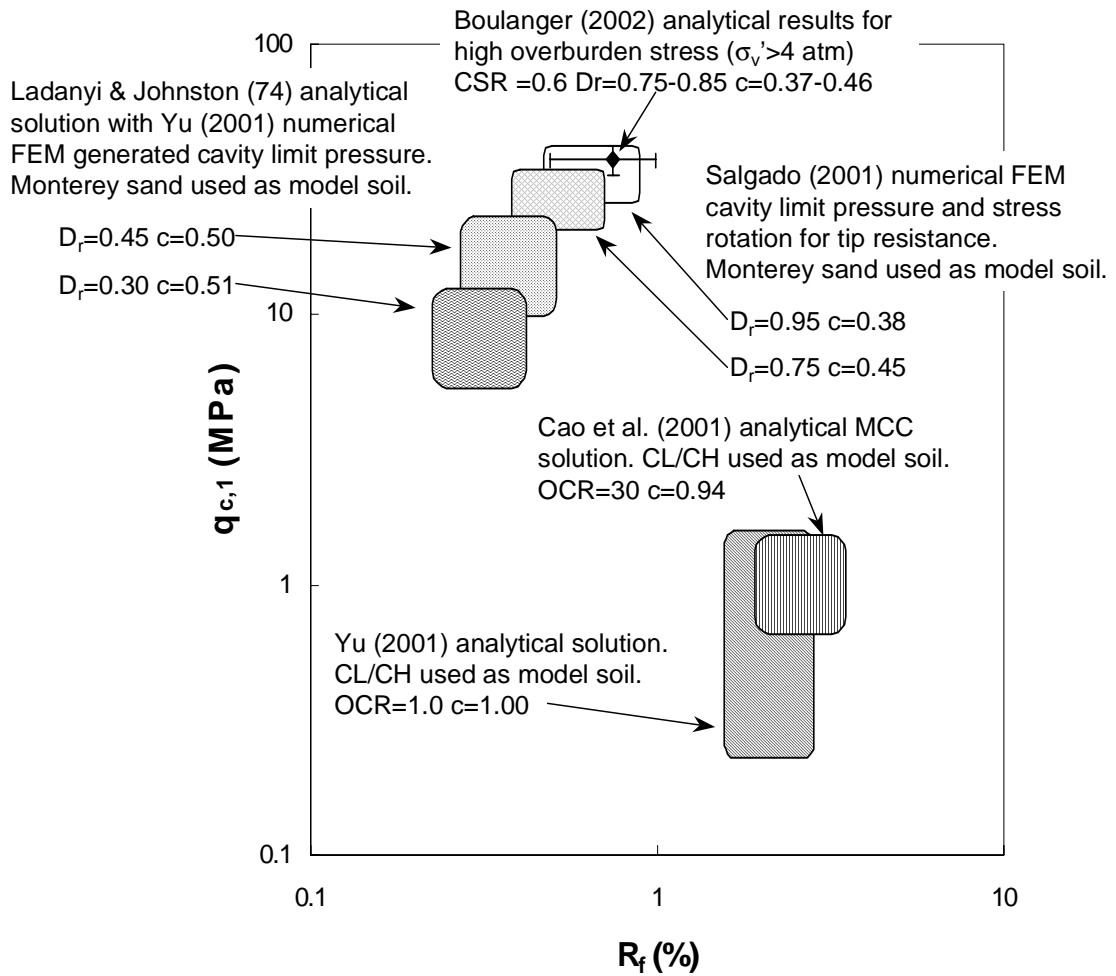


Figure 3.5 Tip Normalization Exponent Results from Cavity Expansion Analyses.

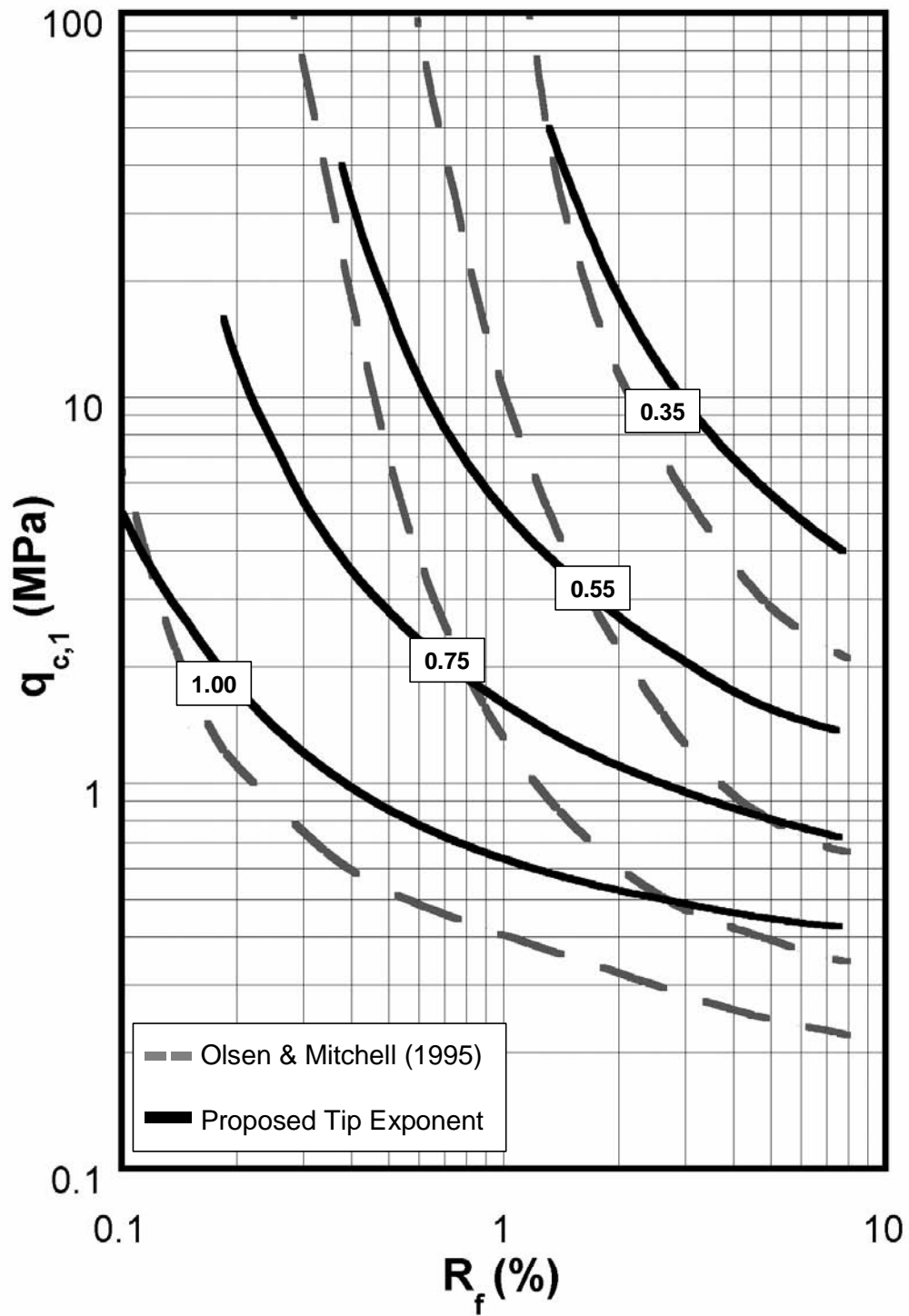


Figure 3.6 Comparison of Proposed Tip Normalization Exponent Contours with Olsen & Mitchell (1995) Tip Normalization Contours.

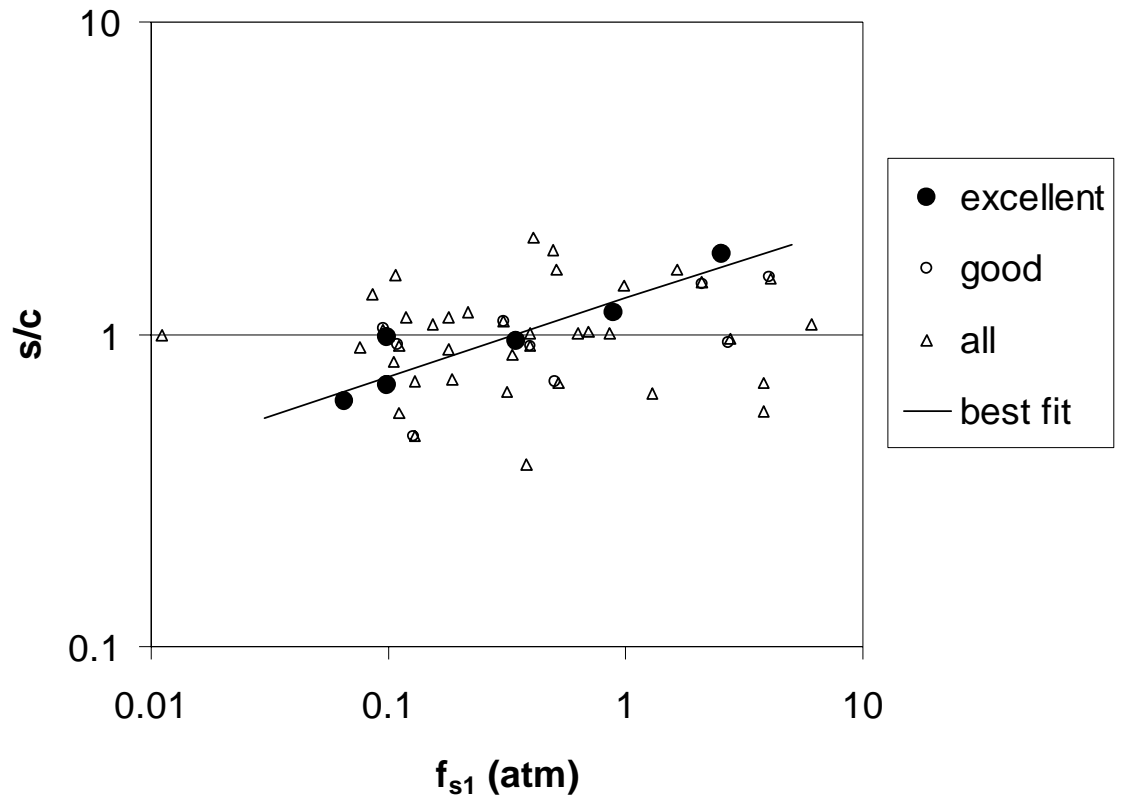


Figure 3.7 Ratio of Sleeve to Tip Normalization Exponents versus Normalized Sleeve Resistance (after Olsen, 1994).

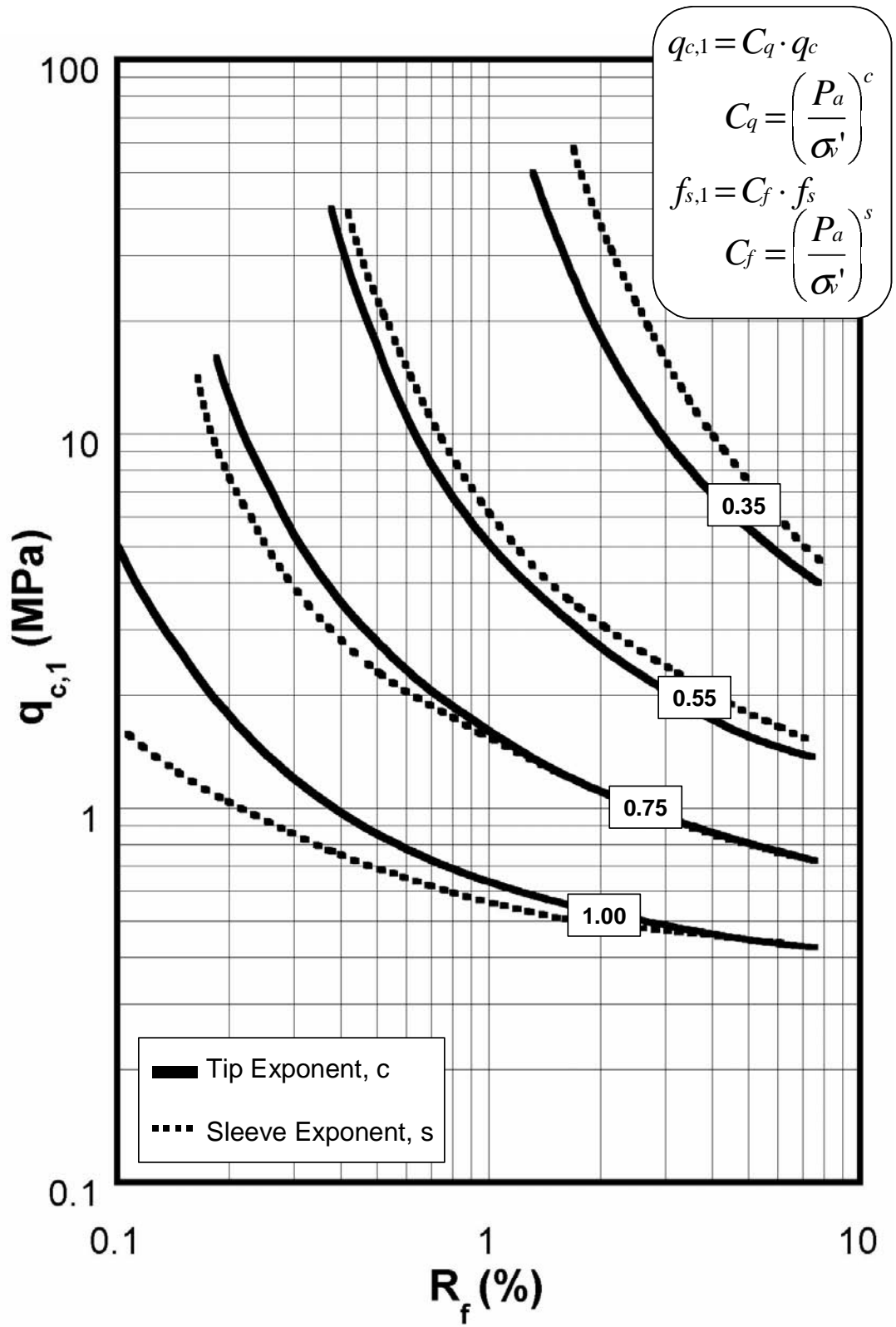


Figure 3.8 Proposed Tip and Sleeve Normalization Exponent Contours.

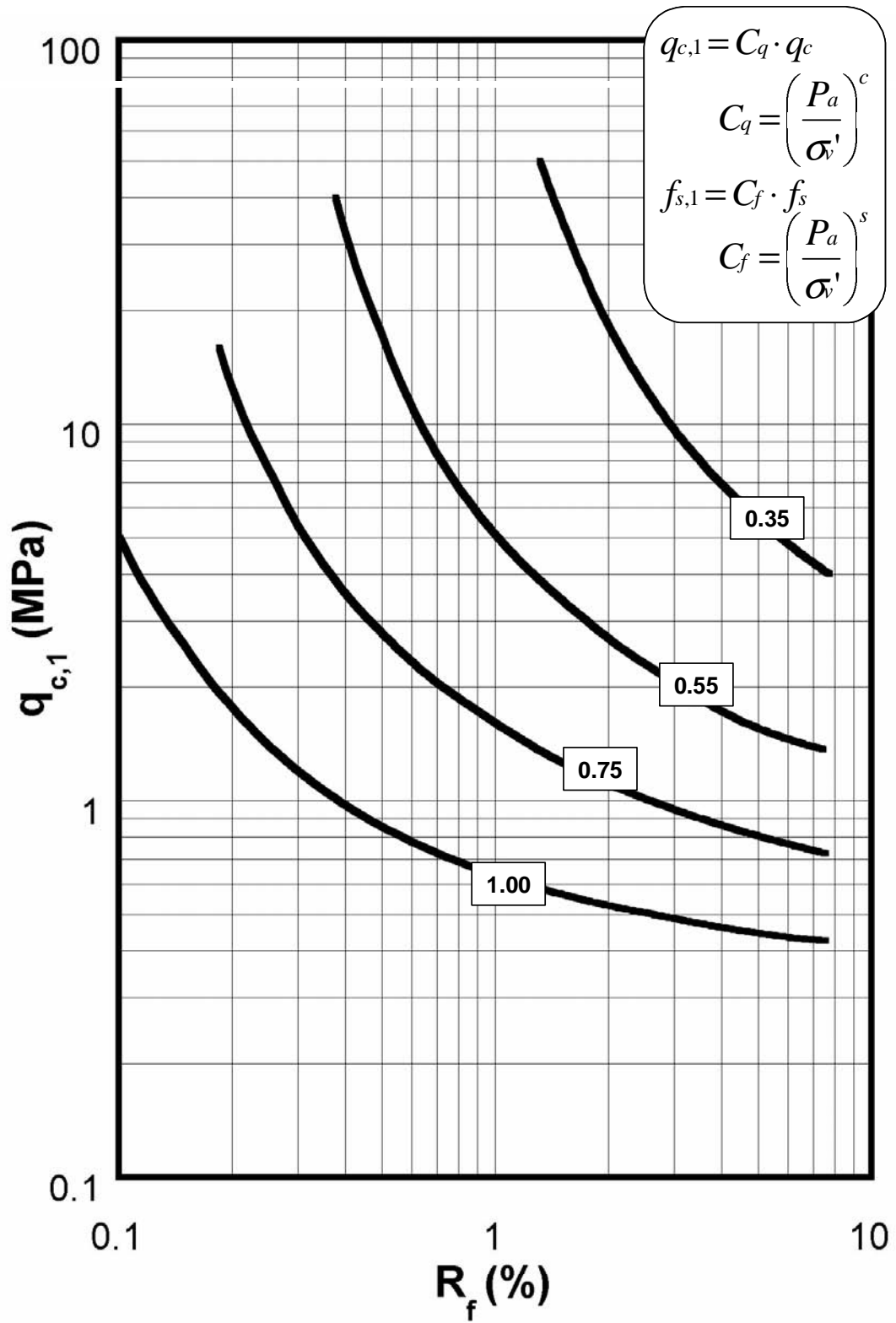


Figure 3.9 Proposed Tip Normalization Exponent Contours.